

## Article

# The Sustained Response of Dissolved Inorganic Carbon to Urban Constructed Wetland in the Fenhe River, China: A Case Study

Jiajia Dang<sup>1</sup>, Meifang Zhang<sup>2</sup> and Yunxiao Li<sup>2,\*</sup> <sup>1</sup> Student Affairs Department, Shanxi Agricultural University, Taigu 030801, China<sup>2</sup> Environmental Science Laboratory, College of Resource and Environment, Shanxi Agricultural University, Taigu 030801, China

\* Correspondence: liyunxiao\_ouc@163.com

**Abstract:** Sustained wetland utilization has been effective in purifying urban riverine pollutants and promoting sustainable development. However, its effect on water CO<sub>2</sub> system remains unclear in semi-arid areas. In this study, seasonal monitoring of the carbonate system was performed at two compared stations, i.e., in constructed wetland (Xiangyun station) and its upstream (Lancun station) in a semi-arid river (the Fenhe River) in China. As indicated by the result of the sustained monthly observation from May 2020 to May 2021, riverine dissolved inorganic carbon (DIC) and partial pressure of CO<sub>2</sub> (*p*CO<sub>2</sub>) reached 30.9–46.7 mg L<sup>-1</sup> and 524–1050 μatm in Lancun station, respectively, whereas the above-described values declined significantly in Xiangyun station with the values of 24.1–39.1 mg L<sup>-1</sup> for DIC and 188–873 μatm for *p*CO<sub>2</sub>. Compared with the Lancun station where the carbonate system was primarily controlled by natural factors (e.g., carbonate weathering and temperature), significant aquatic photosynthesis and calcification precipitation due to constructed wetland triggered the decrease in DIC and *p*CO<sub>2</sub> and dominated their temporal variation in Xiangyun station. Thus, the large CO<sub>2</sub> reduction arising from constructed wetlands may create vital paths for CO<sub>2</sub> neutralization and sustainable conservation in urban rivers in arid and semi-arid areas in the future.

**Keywords:** carbonate system; partial pressure of CO<sub>2</sub>; sustained wetland utilization; aquatic photosynthesis; semi-arid areas



**Citation:** Dang, J.; Zhang, M.; Li, Y. The Sustained Response of Dissolved Inorganic Carbon to Urban Constructed Wetland in the Fenhe River, China: A Case Study. *Sustainability* **2024**, *16*, 1930. <https://doi.org/10.3390/su16051930>

Academic Editor: Miklas Scholz

Received: 14 January 2024

Revised: 7 February 2024

Accepted: 22 February 2024

Published: 27 February 2024



**Copyright:** © 2024 by the authors. Licensee MDPI, Basel, Switzerland. This article is an open access article distributed under the terms and conditions of the Creative Commons Attribution (CC BY) license (<https://creativecommons.org/licenses/by/4.0/>).

## 1. Introduction

The inland river system, i.e., a vital segment connecting the land, ocean and atmosphere, has taken on critical significance in global carbon cycle, annually horizontally transporting ~0.4 Pg inorganic carbon to the ocean and vertically releasing ~1.8 Pg CO<sub>2</sub> to the atmosphere [1–5]. Although extensive research has placed a focus on carbonate systems in big rivers [6–9], optimized and in-depth efforts are required, especially in small watershed rivers with less attention possibly arising from their small volume [10–12]. Moreover, small watershed rivers are more sensitive to rapid urbanization and enhanced land use variations, and the transportation and transformation rates of riverine carbon are faster [13]. Thus, the changes of inorganic carbon system and its control mechanism in small watershed rivers turn out to be more sophisticated.

Compared with big rivers with large freshwater runoff such as Yangtze River or Mississippi River, the effect exerted by anthropogenic disturbance on small watershed rivers may be more prominent for their low runoff and weak environmental capacity [10,14,15]. Notably, in urbanized rivers, industrial or municipal sewage input has significantly worsened the ecological environment and surrounding landscape of the receiving water body [16]. In the lower Han River (South Korea) with high urbanization, Yoon et al. [17] found that wastewater input caused the CO<sub>2</sub> levels in the receiving water increased 4-fold, approaching 8000 μatm. In two small rivers in Chongqing City (China), Wang et al. [11] found

that riverine CO<sub>2</sub> concentration in urban water bodies increased by 2–2.5 times compared to suburban areas. Correspondingly, constructed wetlands have progressively become effective in optimizing urban water environment, and attracted large numbers of studies [18,19]. For example, Scholz et al. [20] found that constructed wetlands would result in a removal of 72% initial nitrate and 35% of initial biological oxygen demand within weeks. Also, wetlands have high efficiency for the removal of PAH and persistent organic pollution [21,22]. Moreover, massive implementation of urban constructed wetland caused enhanced aquatic photosynthesis due to eutrophication [23], which may decrease riverine CO<sub>2</sub> levels and even emerge a potential CO<sub>2</sub> sink in urbanized regions. In an urban tidal marsh in the Huzhou-Raritan estuary, Schäfer et al. [24] assessed the net ecosystem exchange and the maximum rates reached  $-30 \mu\text{mol m}^{-2} \text{s}^{-1}$ . Recently, Wu et al. [25] found that the CO<sub>2</sub> flux of urban wetland in the Xining City in the Qinghai Tibet Plateau showed a net uptake in each month and the maximum value occurred in September. In particular, the achievement of the CO<sub>2</sub> peak and further net-zero CO<sub>2</sub> emissions (i.e., carbon neutrality) followed by the Paris Agreement in 2016 have become a global consensus. In China, the areas of constructed wetland have reached more than 67,000 km<sup>2</sup> [26]. Thus, the effect of urban constructed wetland on carbonate system in the surrounding rivers should be explored, which may help further clear the anthropogenic stressors on inorganic carbon system and achieve more CO<sub>2</sub> absorption in a natural form in urban rivers.

In the arid and semi-arid climate, the rivers on the Loess Plateau in northern China have relatively small discharge compared with the rivers in humid areas, e.g., the discharge of the Yellow River (the sixth longest river in the world) that only takes up 5.0% of Yangtze River and 7.7% of the Mississippi River in humid areas [27,28]. Thus, the human interference in urban expansion may further increase the variation intensity of riverine carbonate system in loess areas. However, the research on riverine carbon transport in the Loess Plateau mainly focused on the main stream of the Yellow River with large runoff [29,30], while the related research in small watersheds especially several small rivers flowing through big cities showed a minor attention. The Fenhe River, the second longest tributary of the Yellow River, offers ~40% water supply in Shanxi Province, China [31], and is deeply affected by human interference. To be specific, when the river drains the capital of Shanxi Province (Taiyuan City), a ~30 km riverside wetland park through rubber damming and artificial planting is conducted for water quality purification, ecological restoration, and landscape enhancement. Thus, it is interesting and important to examine how the riverine inorganic carbon system and CO<sub>2</sub> dynamic have responded to the artificial wetlands. In this study, based on monthly observations over an annual cycle at two stations (one was in urban wetland and the other was in the upstream of wetland), the riverine carbonate system variability and related CO<sub>2</sub> dynamic controls were analyzed to highlight the potential impact of constructed wetland. This study would be helpful to present more insights into the inorganic carbon system and contribute to the prediction of CO<sub>2</sub> trend in urbanized rivers with constructed wetland in semi-arid areas.

## 2. Materials and Methods

### 2.1. Study Area

This study is conducted on Lancun station and Xiangyun station with a distance interval of ~30 km between them. These two stations are in the Taiyuan section of the Fenhe River (112.39° E–112.57° E and 37.61° N–38.02° N, Figure 1), which is in the middle of Shanxi Province, China. The Fenhe River is the second longest tributary of the Yellow River and the largest river in Shanxi Province, which is in the east of the Loess Plateau, with an extensive loess cover. Taiyuan City is the capital of Shanxi Province and has a 5.3 million population and a 65-billion-dollar GDP in 2021.

Lancun station is located in the upstream of Taiyuan City and is an important drinking water source. The river at this station and its upstream expresses as a mountainous river with a karst land type [32] and a good vegetation coverage dominated by forests and grassland (Figure 1). Thus, the river water at Lancun station shows a relatively natural

river background. In comparison, when the river enters the urban zone of Taiyuan City, the river water is gradually stored by about 11 rubber dams or weirs and constructed ecological wetland is implemented for water conservancy regulation, forming a riverside urban park with a width of ~500 m and a length of ~30 km. Xiangyun station is located in the middle of this riverside urban park and it is investigated for analyzing the impact of urban constructed wetland (Figure 1). Dominated by a temperate semi-arid monsoon climate, the study area has an average annual precipitation of ~450 mm and the rainfall in summer accounts for >60% proportion.

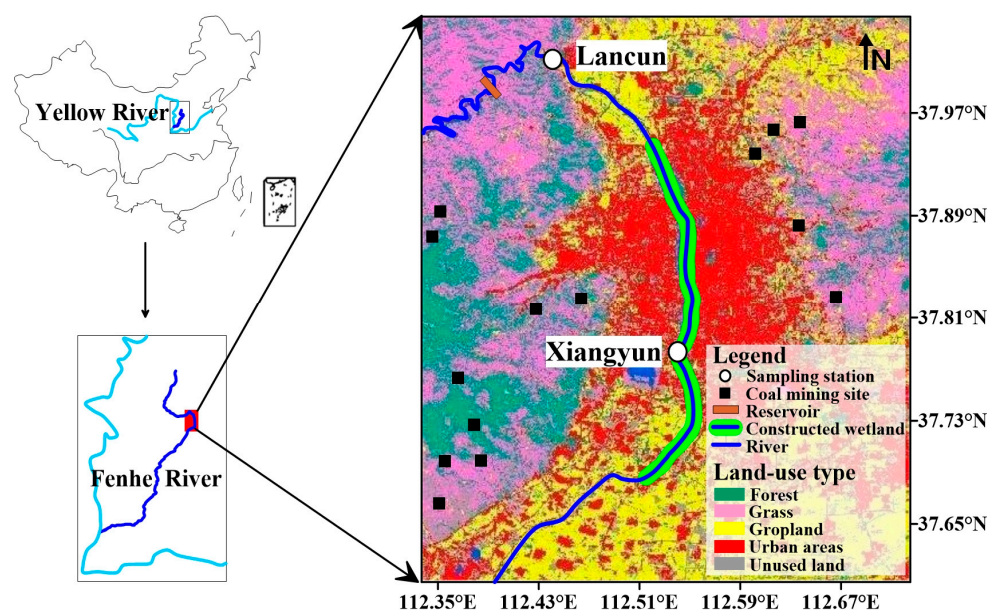


**Figure 1.** Study area and sampling station map. Note that this figure shows the riverside constructed wetland area in Taiyuan City, coal mining sites and land-use type of study area.

## 2.2. Station Setting and Sample Processing

For this study, monthly observations over an annual cycle were conducted in Lancun station as background station and Xiangyun station in urban constructed wetland (Figure 1) from May 2020 to May 2021, and thus 13 observations were obtained in each station. During each month, the sampling work was carried out on sunny days and near mid-day, and water sample at a depth of ~0.2 m in the middle of the riverbed was obtained at these two stations using a plexiglass vertical water sampler. After collecting the water sample on site, dissolved oxygen saturation (DO%) were determined immediately, and then the samples of riverine ions, dissolved inorganic carbon (DIC) and its stable carbon isotope ( $\delta^{13}\text{C}_{\text{DIC}}$ ) were filtrated. pH samples were determined in the laboratory within 8 h after sampling (Table 1). Also, the parallel double samples were collected for DIC,  $\delta^{13}\text{C}_{\text{DIC}}$ , pH and ions parameters, and their average values were adopted in this study due to the minor concentration differences between the parallel double samples.

**Table 1.** Riverine water chemistry and concentrations of DIC,  $\delta^{13}\text{C}_{\text{DIC}}$ , DOC and  $p\text{CO}_2$  in two investigated stations over an annual cycle.

Location	Sample	$T_w$ °C	pH	AOU $\mu\text{mol kg}^{-1}$	DIC $\text{mg L}^{-1}$	$\delta^{13}\text{C}_{\text{DIC}}$ ‰	DOC $\text{mg L}^{-1}$	$p\text{CO}_2$ $\mu\text{atm}$	$\text{Ca}^{2+}$ $\text{mmol L}^{-1}$	$\text{Mg}^{2+}$ $\text{mmol L}^{-1}$
Lancun	Max	22.4	8.55	−60.1	46.7	−5.51	5.40	1050	2.01	1.36
	Min	0.3	8.29	−4.2	30.9	−6.98	3.16	524	1.46	1.06
	Average	11.4	8.39	−23.6	38.1	−6.31	4.37	722	1.68	1.16
	SD	7.8	0.08	16.1	5.2	0.39	0.73	151	0.17	0.08
Xiangyun	Max	27.4	8.86	−121.7	39.1	−2.10	11.77	873	1.86	1.29
	Min	2.2	8.33	−1.2	24.1	−6.54	3.62	188	1.03	0.74
	Average	13.9	8.52	−40.9	34.5	−4.94	6.99	519	1.57	1.16
	SD	9.1	0.13	41.3	5.0	1.48	2.88	193	0.26	0.13

Water temperature ( $T_w$ ) and DO% were determined via a YSI oxygen analyzer (Pro20i, YSI Corporation, Yellow Spring, OH, USA), and the Winkler titration method was also applied for DO calibration (nominal precision: 0.1%). Then, apparent oxygen utilization (AOU) was calculated via saturated DO concentration in river minus the observed DO concentration [33]. AOU has been reported as a vital indicator of biological production or community respiration [10,34–36], i.e., negative AOU suggests the dominance of biological production and positive AOU corresponds to the dominance of community respiration. pH samples were collected in 150 mL polytetrafluoroethylene bottles and sealed to avoid bubbles, and they were measured at 25 °C ( $pH_{@25^\circ C}$ ) in the laboratory using a pH Benchtop Meter (FE28, Mettler Toledo Corporation, Switzerland) with a precision of  $\pm 0.01$ , and the NBS (pH = 4.01, 7.00, and 9.21 at 25 °C) buffers were used for pH measurements. DIC and  $\delta^{13}C_{DIC}$  samples were filtered to 20 mL high borosilicate glass bottles with 0.45  $\mu m$  disposable syringe filters and dissolved organic carbon (DOC) samples were filtered through 0.7  $\mu m$  GF/F glass fiber membrane (Whatman Corporation, Maidstone, UK) into 100 mL vials, and then these samples were stored at 4 °C until laboratory analysis after addition of saturated mercuric chloride solution (final concentration:  $\sim 0.04\%$  by volume). The concentrations of DIC and DOC were measured by using a total organic carbon analyzer (Multi N/C 3100, Analytik Jena Corporation, Jena, Germany) with an uncertainty of  $\sim 0.06 \text{ mg L}^{-1}$  [37]. The  $\delta^{13}C_{DIC}$  values were measured using a Gasbench II Extraction Line coupled with a Finnigan MAT 253 Mass Spectrometer (Thermo Electron Corporation, Massachusetts, USA), with a standard deviation of 0.05‰ ( $n = 4$ ).  $Ca^{2+}$  and  $Mg^{2+}$  samples were filtered in 125 mL polytetrafluoroethylene bottles with 0.45  $\mu m$  cellulose acetate membranes, and their concentrations were determined by using an Ion Chromatography (HIC-20Asuper, Shimadzu Corporation, Kyoto, Japan) with uncertainties of 5%. The above instrument analysis work was completed within three weeks after sampling. Also, *in situ* pH, partial pressure of  $CO_2$  ( $pCO_2$ ) and  $[HCO_3^-]$  were calculated from DIC,  $pH_{@25^\circ C}$  and  $T_w$  based on the CO2SYS program (Version 2.3) [38] which was a calculator for the  $CO_2$  system for Microsoft Excel 2016 and was used in many studies [35–37,39]. The dissociation constants ( $K_1$  and  $K_2$ ) of carbonic acid determined by Millero. (1979) [40] were used.

### 2.3. Simulation of $pCO_2$ Change Due to Temperature Effect and Biological Production

#### 2.3.1. Temperature Effect

Temperature could affect the concentration and proportion of carbonate components, causing  $pCO_2$  change through changing the dissociation degree of  $H_2O$  and  $HCO_3^-$  at a constant total alkalinity (TA) and DIC level [35,36,38,39]. Thus, the contribution of temperature effect to  $pCO_2$  changes ( $\Delta pCO_{2Tem}$ ) is calculated via Equation (1) based on the CO2SYS program.

$$\Delta pCO_{2Tem} = p(DIC_i, TA_i, T_{w_i} + \Delta T_w) - pCO_{2i} \quad (1)$$

where  $DIC_i$ ,  $TA_i$ ,  $T_{w_i}$  and  $pCO_{2i}$  represent DIC, TA, water temperature and  $pCO_2$  for the calculation starting point, respectively.  $\Delta T_w$  indicated the temperature change. TA was computed by pH and DIC.

Also, to remove the effect exerted by temperature, through Equation (1) *in situ*  $pCO_2$  could be normalized to a constant temperature, such as the annual average temperature, and thus  $npCO_2$  could be obtained.

#### 2.3.2. Biological Production

Based on the classic Redfield stoichiometry of DIC: AOU = 106:138 [41], the changes of DIC caused by biological production ( $\Delta DIC_{Bio}$ ) could be calculated through Equation (2) based on the AOU difference ( $\Delta AOU$ ):

$$\Delta DIC_{Bio} = \Delta AOU / 138 \times 106 \quad (2)$$

Thus, the changes of  $p\text{CO}_2$  caused biological production ( $\Delta p\text{CO}_{2\text{Bio}}$ ) could be computed via Equation (3):

$$\Delta p\text{CO}_{2\text{Bio}} = p(\text{DIC}_i + \Delta\text{DIC}_{\text{Bio}}, \text{TA}_i, T_w i) - p\text{CO}_{2i} \quad (3)$$

#### 2.4. Statistical Analysis

The correlations tests in the investigated parameters were analyzed using a SPSS 17.0 software (IBM Corporation, New York, NY, USA). Statistical analysis was considered significant at the level of  $p < 0.05$ .

### 3. Results

#### 3.1. Variations of Water Chemistry

As depicted in Table 1, over an annual cycle from May 2020 through May 2021,  $T_w$  was 0.3–22.4 °C in Lancun station and 2.2–27.4 °C in Xiangyun station, and a minor difference was reported in the annual mean  $T_w$  between the above-mentioned two stations (11.4 °C vs. 13.9 °C). The river water was mildly alkaline, and *in situ* pH values ranged from 8.29 to 8.55, with a mean of 8.39 in Lancun station. However, in Xiangyun station located in urban constructed wetland, the pH values were elevated notably with a range between 8.33 and 8.86 (average 8.52). AOU values in both of the above-described two stations over an entire year were negative, showing the dominance of biological production. In Lancun station, DO was slightly supersaturated with an average AOU of  $-23.6 \pm 16.1 \mu\text{mol kg}^{-1}$ . In contrast, in Xiangyun station the degree of DO supersaturation was notably increased with an average AOU of  $-40.9 \pm 41.3 \mu\text{mol kg}^{-1}$  (Figure 2b), suggesting a significant aquatic photosynthesis. The mole concentration of  $\text{Ca}^{2+}$  reached  $1.68 \pm 0.17 \text{ mmol L}^{-1}$  in Lancun station, and it declined in Xiangyun station, with a mean of  $1.57 \pm 0.26 \text{ mmol L}^{-1}$ . The mole concentration of  $\text{Mg}^{2+}$  was 1.06–1.36  $\text{mmol L}^{-1}$  in Lancun station and 0.74–1.29  $\text{mmol L}^{-1}$  in Xiangyun station (Table 1).

#### 3.2. Variations of Riverine DIC, DOC, $\delta^{13}\text{C}_{\text{DIC}}$ and $p\text{CO}_2$

Riverine DIC concentrations in Lancun station varied widely from 30.9  $\text{mg L}^{-1}$  to 46.7  $\text{mg L}^{-1}$ , with a mean of 38.1  $\text{mg L}^{-1}$  (Table 1, Figure 2). Temporally, high DIC ( $>45 \text{ mg L}^{-1}$ ) was primarily reported in high-runoff and cold months (e.g., January and February), and low DIC ( $<35 \text{ mg L}^{-1}$ ) in low-runoff and warm months (e.g., July–October). In comparison, Xiangyun station achieved a lower DIC concentration ranging from 24.1  $\text{mg L}^{-1}$  to 39.1  $\text{mg L}^{-1}$ , with a mean of 34.5  $\text{mg L}^{-1}$ , and especially during warm July–October DIC concentration was even below 30  $\text{mg L}^{-1}$ . Riverine  $\delta^{13}\text{C}_{\text{DIC}}$  concentration in Lancun station varied from  $-6.98\%$  to  $-5.51\%$  with a mean of  $-6.31\%$ , showing a minor temporal variation. However, in Xiangyun station, riverine  $\delta^{13}\text{C}_{\text{DIC}}$  changed widely with a range of  $-6.54\%$  to  $-2.10\%$  and showed a more enriched average concentration ( $-4.94\%$ ). Temporally, compared with Lancun station, the enriched  $\delta^{13}\text{C}_{\text{DIC}}$  mainly appeared in warm months (e.g., July–October) with the concentration of  $>-4.50\%$ . The DOC concentration was  $4.37 \pm 0.73 \text{ mg L}^{-1}$  in Lancun station and it increased to  $6.99 \pm 2.88 \text{ mg L}^{-1}$  in Xiangyun station. Temporally, the obvious increase in DOC also mainly showed in warm months (e.g., July–October) with the concentration of  $>8.50 \text{ mg L}^{-1}$  in Xiangyun station. Riverine  $p\text{CO}_2$  in Lancun station was supersaturated for atmospheric  $\text{CO}_2$  on an annual cycle, ranging between 524  $\mu\text{atm}$  and 1050  $\mu\text{atm}$ , with a mean of 722  $\mu\text{atm}$ . Besides, it generally declined from June to January and then rose to May of the next year. Riverine  $p\text{CO}_2$  in Xiangyun station varied from 188  $\mu\text{atm}$  to 873  $\mu\text{atm}$ , with a mean of 519  $\mu\text{atm}$ . Temporally, compared with Lancun station,  $p\text{CO}_2$  during November–May achieved a small decrease of  $\sim 90 \mu\text{atm}$ , and it was also supersaturated for atmospheric  $\text{CO}_2$ . However,  $p\text{CO}_2$  during warm months (i.e., July–October) displayed a large reduction of  $>400 \mu\text{atm}$  with the minimum value of 188  $\mu\text{atm}$ , and the river acted as an atmospheric  $\text{CO}_2$  sink.

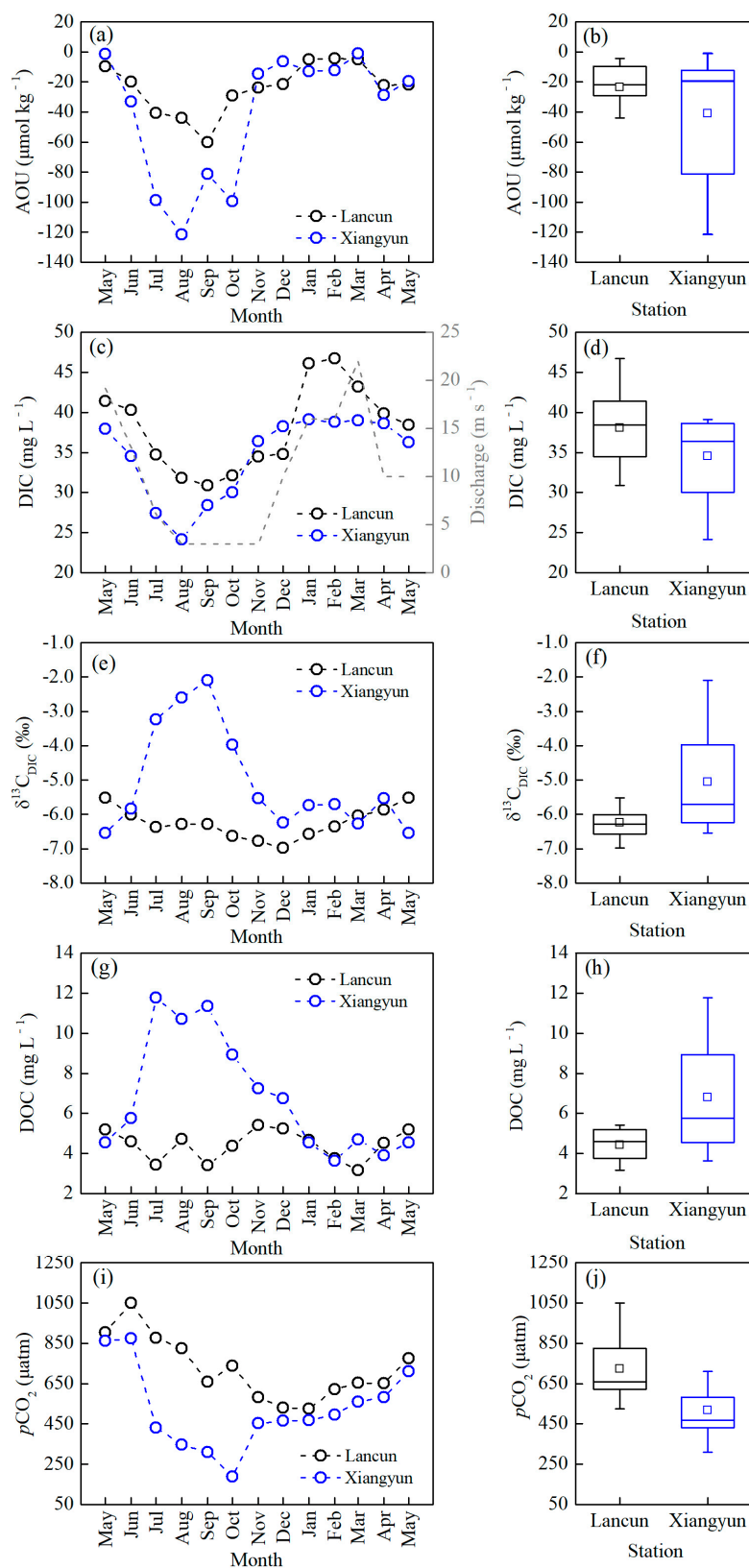


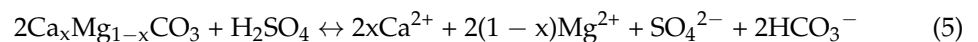
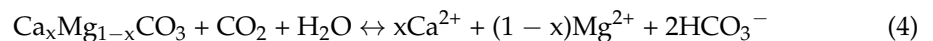
**Figure 2.** Monthly variations of riverine AOU (a), DIC (c) and  $p\text{CO}_2$  (i) in Lancun station (black circles) and Xiangyun station (blue circles) from May 2020 through May 2021 and the boxplots describing the yearly AOU (b), DIC (d) and  $p\text{CO}_2$  (j) concentrations. In panel (c), the grey dashed line denotes river discharge at Lancun station. Also, the monthly riverine  $\delta^{13}\text{C}_{\text{DIC}}$  (e,f) and DOC (g,h) concentration from January 2021 to December 2021 are showed.

## 4. Discussion

### 4.1. The Controls of DIC Variation at Background Station

Generally, the chemical weathering of rocks in the basin could convert atmospheric CO<sub>2</sub> and C (carbonate) contained in rocks into HCO<sub>3</sub><sup>−</sup> in river water, which is the main source of DIC in natural rivers [6,27,42,43]. Meanwhile, compared with granite rocks, the weathering rate of carbonate rocks is 12 times faster [44], and thus its effect on riverine DIC has been widely reported [10,42,45]. In this study, Lancun station as background station is the important drinking water source of Taiyuan City with a better vegetation coverage (Figure 1), and both banks of its upstream are dominated by rock mountain area characterized by Ordovician limestone (carbonate rocks) with little silicate cover [32]. Thus, carbonate weathering would be an important cause for the high annual DIC concentration (38.1 ± 5.2 mg L<sup>−1</sup>) at Lancun station.

In carbonate weathering, carbonate rocks are usually predominantly dissolved by H<sub>2</sub>CO<sub>3</sub>. In this process, the δ<sup>13</sup>C value of soil CO<sub>2</sub> dissolved in water should be −17‰ for C3 plants, and marine carbonate δ<sup>13</sup>C has more enriched value with an average of ~0‰ [46–48]. Thus, half of total DIC is derived from carbonate rocks and the other half from soil CO<sub>2</sub>, producing a 1:2 molar ratio of [Ca<sup>2+</sup> + Mg<sup>2+</sup>]/[HCO<sub>3</sub><sup>−</sup>] with a δ<sup>13</sup>C value of −8.5‰ according to Equation (4) due to the minor effect of CO<sub>2</sub> degassing. However, when carbonate rocks are weathered by H<sub>2</sub>SO<sub>4</sub>, total DIC is 100% derived from minerals, producing a 1:1 molar ratio of [Ca<sup>2+</sup> + Mg<sup>2+</sup>]/[HCO<sub>3</sub><sup>−</sup>] with an enriched δ<sup>13</sup>C value of 0‰ according to Equation (5):



As depicted in Figure 3a and Table 1, the mole ratios of [Ca<sup>2+</sup>+Mg<sup>2+</sup>]/[HCO<sub>3</sub><sup>−</sup>] at Lancun station as background station notably ranged from 1 to 0.5, and the δ<sup>13</sup>C<sub>DIC</sub> value (−6.98‰~−5.51‰) was also between −8.5‰ and 0‰. It was suggested that riverine DIC at this station primarily originated from carbonate weathering involved by H<sub>2</sub>CO<sub>3</sub> and H<sub>2</sub>SO<sub>4</sub>. Moreover, the above finding was confirmed by the equivalent ratio of [Ca<sup>2+</sup>+Mg<sup>2+</sup>]/[HCO<sub>3</sub><sup>−</sup>+SO<sub>4</sub><sup>2−</sup>] that was generally distributed around 1:1 line (Figure 3b). It is noteworthy that the participation of H<sub>2</sub>SO<sub>4</sub> may arise from the extensive exploitation of coal resources with considerable SO<sub>4</sub><sup>2−</sup> [32]. Numerous coal mining sites were close to the study area (Figure 1). Moreover, the annual volume of coal mining in Shanxi Province in 2019 where the study station was located reached 9.9 × 10<sup>8</sup> tons, taking up 26% of China's total coal output [49]. Likewise, in two small karst catchments in Chongqing City (China) with high-sulfur (3.2%) coal as an energy resource, Zhang et al. [50] reported the significant involvement of H<sub>2</sub>SO<sub>4</sub> in carbonate weathering. Thus, temporally, the intensity of carbonate weathering would determine the annual change of DIC at Lancun station. River discharge is an important factor for the chemical weathering rate of rocks. High flow accompanied by significant erosion process will promote more weathering products to enter the river, thus leading to the increase in riverine DIC [9,51]. As depicted in Figure 4, riverine DIC at Lancun station showed a significant positive correlation with riverine discharge, and high DIC values accompanied with high discharge. Moreover, the determination coefficient (r<sup>2</sup>) reached 0.78, suggesting that at least 78% monthly variation of DIC could be explained by river discharge. Note that river discharge at Lancun station is mainly controlled by reservoir regulation due to the existence of Fenhe Reservoir II with a 88 m height dam at its upstream (Figure 1) though river discharge variation is always closely related to rainfall which usually brings dilution effect and reduces the concentration of ions in the river [12,43]. Therefore, in Lancun station the high discharge did not occur in summer with more rainfall and the magnitude of reservoir-affected discharge corresponded to the intensity of erosion process. As for the biological activities, it may have a minor effect on DIC temporal variation in Lancun station, considering the near-equilibrium DO (107.6% ± 6.0%) and minor monthly changes in the DOC (4.37 ± 0.73 mg L<sup>−1</sup>) and

$\delta^{13}\text{C}_{\text{DIC}}$  ( $-6.30\text{‰} \pm 0.39\text{‰}$ ) in this entire year cycle (Figure 2, Table 1). Overall, carbonate weathering involved by  $\text{H}_2\text{CO}_3$  and  $\text{H}_2\text{SO}_4$  resulted in the high DIC levels at Lancun station as background station, and weathering intensity was mainly affected by river discharge.

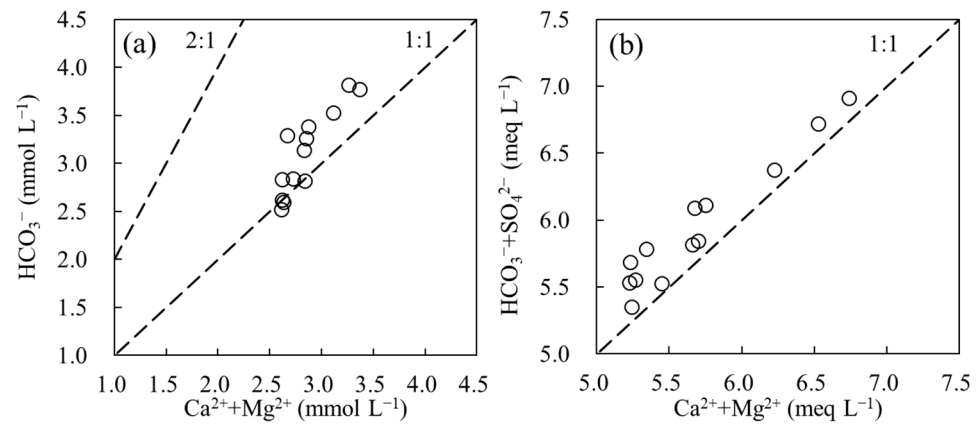


**Figure 3.** Variations in molar  $[\text{HCO}_3^-]$  versus  $[\text{Ca}^{2+} + \text{Mg}^{2+}]$  ratio (a), and equivalent  $[\text{HCO}_3^- + \text{SO}_4^{2-}]$  versus  $[\text{Ca}^{2+} + \text{Mg}^{2+}]$  ratio (b) at Lancun station over an annual cycle from May 2020 to May 2021.

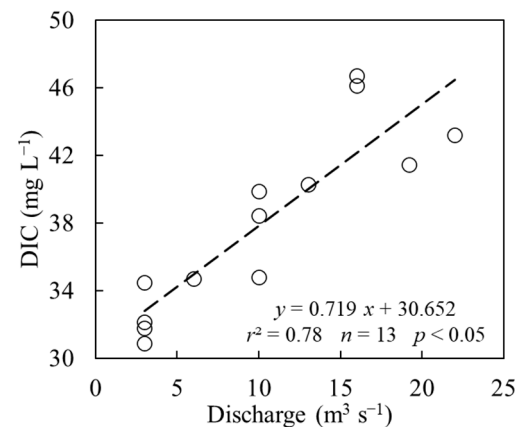


**Figure 4.** Correlation of DIC and water discharge at Lancun station over an annual cycle from May 2020 to May 2021.

#### 4.2. The Effect of Urban Constructed Wetland on Riverine DIC

Compared with Lancun station at the urban upstream, the river is gradually closed with  $\sim 11$  dams or weirs when it flows into Taiyuan City, forming a riverside wetland park with a  $\sim 30$  km length and  $\sim 500$  m width, and Xiangyun station is located in the middle of the riverside wetland park. From May 2020 to May 2021, the DIC concentrations at Xiangyun station ( $24.1\text{--}39.1$   $\text{mg L}^{-1}$ ) were generally lower than those ( $30.9\text{--}46.7$   $\text{mg L}^{-1}$ ) at Lancun station in the respective month, and in warm summer the DIC even decreased by  $>20\%$ , suggesting that some processes notably reducing DIC were existed in Xiangyun station (Figure 2).

In general, the non-free flowing water body is easy to be autotrophic, due to the accumulation of nutrients and stable water conditions; the free-flowing water body tends to be a slightly heterotrophic or biological balanced status [52–54]. Aquatic photosynthesis could consume a large amount of  $\text{CO}_2$  and preferentially absorb  $^{12}\text{C}$  in the river, leading to the decrease in DIC and a more positive  $\delta^{13}\text{C}_{\text{DIC}}$ . Compared with Lancun station with well fluidity ( $10.3 \pm 6.3$   $\text{m}^3 \text{s}^{-1}$ ) and near-equilibrium DO ( $107.6\% \pm 6.0\%$ ) (Figure 2, Table 1), wider riverbed and more static water body induced by the closure of the dams would facilitate the photosynthesis of plankton. DO at Xiangyun station was notably supersaturated all year round with an average DO% of  $114.3\% \pm 15.7\%$  and showed a more enriched  $\delta^{13}\text{C}_{\text{DIC}}$  value of  $-4.94\text{‰} \pm 1.48\text{‰}$ . This indicated that a strong biological

production appeared in Xiangyun station, and the large biological CO<sub>2</sub> consumption would be an important factor for the decrease in DIC. Moreover, both AOU and  $\delta^{13}\text{C}_{\text{DIC}}$  showed significant positive correlations with DIC (Figure 5a,b), suggesting that aquatic photosynthesis dominated the DIC monthly variability. Especially in warm July–October, AOU was below  $-80 \mu\text{mol kg}^{-1}$  with the  $\delta^{13}\text{C}_{\text{DIC}}$  of  $>-4.50\text{‰}$  and thus DIC reached the minimum level ( $<30 \text{mg L}^{-1}$ ). Also, the obvious control of aquatic production was shown on the variation of DOC which could indicate the organic matter produced in primary production. Compared with Lancun station, DOC in Xiangyun station increased by 60% with a value of  $6.99 \pm 2.88 \text{mg L}^{-1}$  (Figure 2h), and showed a good positive correlation with  $\delta^{13}\text{C}_{\text{DIC}}$  (Figure 5c). Similarly, this decrease in riverine DIC caused by aquatic photosynthesis was widely found in several river-reservoir systems [51,55,56].

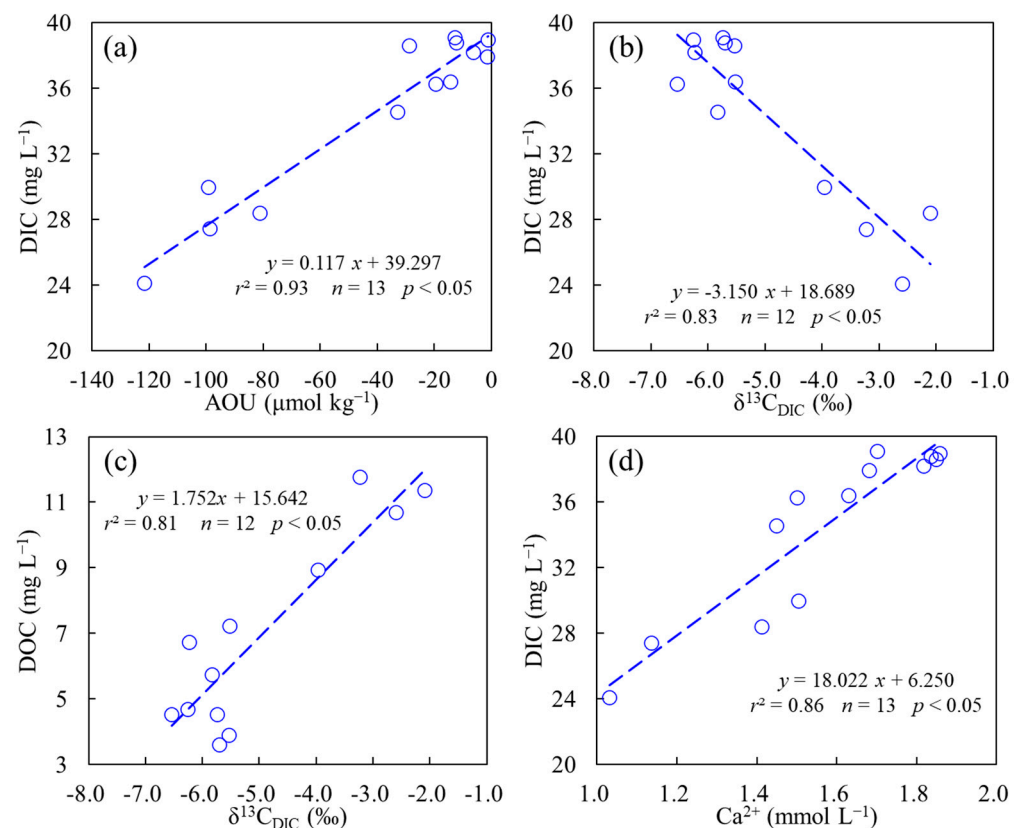


**Figure 5.** Correlations of DIC vs. AOU (a), DIC vs.  $\delta^{13}\text{C}_{\text{DIC}}$  (b), DOC vs.  $\delta^{13}\text{C}_{\text{DIC}}$  (c) and DIC versus Ca<sup>2+</sup> (d) at Xiangyun station. Note that the data of  $\delta^{13}\text{C}_{\text{DIC}}$  and DOC is from January 2021 to December 2021.

As revealed by natural observations and experimental studies, biological production is one of the vital reasons for inducing calcite precipitation which can also result in a significant DIC decrease [57–60]. In other words, significant aquatic photosynthesis can consume considerable CO<sub>2</sub> and increase pH, causing the decrease in the solubility of calcite and the occurrence of calcite precipitation. In Xiangyun station dominated by aquatic photosynthesis, riverine pH reached  $8.52 \pm 0.13$  with high calcium carbonate saturation state ( $>1$ ). As depicted in Figure 5d, Ca<sup>2+</sup> displayed a significant positive correlation with DIC, and low DIC values accompanied with low Ca<sup>2+</sup>, suggesting the important control of calcite precipitation on DIC monthly variation. Similar situations also showed in Ichetucknee River in USA [61], Wujiang [56] and Pearl River in China [62].

Additionally, the changes in water flow at the upstream Lancun station may still affect the hydrological conditions of the wetland area, though the water body of Xiangyun station tends to become stationary due to the layer-by-layer interception of the rubber dams. At the Lancun station, the discharge in summer was at its lowest throughout the

year (Figure 2), which indicated that the water in the downstream wetland area was less affected by fluctuations from upstream inflow. Thus, more stable water structure would facilitate the growth of planktonic algae. This may also be one of the reasons for the lowest AOU and DIC during summer at Xiangyun station. In comparison, in autumn and early winter, the flow rate at Lancun station was the highest (Figure 2), suggesting that the stable hydrological structure of the downstream wetland area was more susceptible to damage. During this period, the AOU and DIC of Xiangyun station were the highest, and the weak biological production were shown. Meanwhile, the rainfall may also affect algal activities in constructed wetland and resulted in the changes in DIC and  $\text{CO}_2$ . Especially in summer, rainfall may bring more nutrient inputs and some trace elements such as Fe and Mn [63,64], promoting the growth of planktonic algae and resulting in the lower AOU and DIC. Overall, in Xiangyun station, significant aquatic photosynthesis and calcification precipitation were the main factors for the decrease in DIC and dominated DIC seasonality.

#### 4.3. The Effect of the Urban Constructed Wetland on Riverine $p\text{CO}_2$ Variability

Riverine  $p\text{CO}_2$ , i.e., the dissolved  $\text{CO}_2$  component in DIC, directly affects the  $\text{CO}_2$  source/sink pattern for the atmosphere in rivers. When the riverine  $p\text{CO}_2$  exceeds the atmospheric  $\text{CO}_2$ , the river will act as a  $\text{CO}_2$  source and vice versa (sink). In this study, the controls of riverine  $p\text{CO}_2$  between Lancun station and Xiangyun station were compared, highlighting the effect of urban constructed wetland.

In general, temperature is a vital factor for  $p\text{CO}_2$  variability. Thermodynamically, the rise of temperature will lead to an increase in riverine  $p\text{CO}_2$  by increasing the dissociation degree of  $\text{H}_2\text{O}$  and  $\text{HCO}_3^-$ , showing a positive correlation between  $p\text{CO}_2$  and  $T_w$  [65]. On average, annual average  $T_w$  only displayed a minor variation between Lancun station ( $11.4^\circ\text{C}$ ) and Xiangyun station ( $13.9^\circ\text{C}$ ), suggesting that temperature was not the dominant factor for the large annual  $p\text{CO}_2$  difference between the above-mentioned two stations ( $722\ \mu\text{atm}$  vs.  $519\ \mu\text{atm}$ ) (Table 1, Figure 2j). However, in monthly variation, the temperature effect was not ignored due to the significant  $T_w$  seasonality. In this study, to obtain the temperature effect on the monthly variability of  $p\text{CO}_2$ , the values ( $T_w$ , DIC,  $p\text{CO}_2$ ) in May 2020 served as the starting point of calculation, and  $p\text{CO}_2$  monthly variation which was purely resulted from temperature effect was simulated based on CO2SYS program and represented by the red dashed lines in Figure 6a,b (See the Equation (1) in Section 2.3.1). As indicated by the results, the simulated *in situ*  $p\text{CO}_2$  value at Lancun station generally was in good agreement with their respective observation in the respective month (Figure 6a) except for the warm July–September months. Meanwhile, from January with minimum  $p\text{CO}_2$  ( $524\ \mu\text{atm}$ ) to June with highest  $p\text{CO}_2$  ( $1050\ \mu\text{atm}$ ), the estimated  $p\text{CO}_2$  variation ( $604\ \mu\text{atm}$ ) arising from the temperature effect only deviated by 15% with the identified  $p\text{CO}_2$  difference ( $526\ \mu\text{atm}$ ). As revealed by the above results, temperature effect may dominate monthly variation of  $p\text{CO}_2$  in Lancun station. In contrast, in Xiangyun station, the simulated  $p\text{CO}_2$  value notably deviated from their respective observation in most months (Figure 6b), suggesting a minor effect from temperature and highlighting the significance of non-temperature processes. In the following, to remove the effect exerted by temperature on the monthly variation of  $p\text{CO}_2$ , *in situ*  $p\text{CO}_2$  would be normalized to the annual average temperature ( $11.4^\circ\text{C}$  in Lancun and  $13.9^\circ\text{C}$  in Xiangyun) of the corresponding station, and  $np\text{CO}_2$  was obtained to explore the effect of biological processes in depth.

Biological production will consume  $\text{CO}_2$  and release oxygen, such that  $p\text{CO}_2$  can be decreased, and DO can be supersaturated (negative AOU). In contrast, community respiration will cause an increased  $p\text{CO}_2$ , unsaturating DO (positive AOU). As depicted in Table 1 and Figure 2a, over an annual cycle from May 2020 to May 2021, DO in two investigated stations was supersaturated, and the biological production turned out to be dominant. Moreover, compared with Lancun station ( $-23.6 \pm 16.1\ \mu\text{mol kg}^{-1}$ ), Xiangyun station displayed stronger aquatic photosynthesis, which was demonstrated by the lower and more negative AOU ( $-40.9 \pm 41.3\ \mu\text{mol kg}^{-1}$ ). First, we simulated the contribution

of biological production to the  $p\text{CO}_2$  change between these two stations. Based on the Equations (2) and (3) in Section 2.3.2, annual average values ( $T_w$ , AOU, DIC,  $p\text{CO}_2$ ) in Lancun station served as the calculation starting point, and the  $p\text{CO}_2$  decrease solely to biological production would be  $142 \mu\text{atm}$ , taking up 70% of the identified difference ( $203 \mu\text{atm}$ ) between the above-described two stations. This indicated that aquatic photosynthesis would serve as the dominant factor for the significant decrease in  $p\text{CO}_2$  at Xiangyun station. Second, temporally, with the aim of analyzing the biological effect on monthly variation of  $p\text{CO}_2$  for each station, the values (AOU, DIC,  $np\text{CO}_2$ ) in May 2020 served as the starting point of calculation, and  $np\text{CO}_2$  monthly variation was estimated, which was solely induced by the biological effect and represented as the black dashed lines in Figure 6c,d. As indicated by the results, the simulated  $np\text{CO}_2$  value in the above-mentioned two investigated stations was generally consistent with their respective observation in the respective month (Figure 6c,d). The results suggested that aquatic photosynthesis also took on critical significance in monthly variation of  $p\text{CO}_2$  in Lancun station though the dominant of temperature effect. Especially during warm July–September with AOU values of  $< -40 \mu\text{mol kg}^{-1}$ , aquatic photosynthesis resulted in the significant decrease in  $p\text{CO}_2$ , primarily accounting for the negative deviation of *in situ*  $p\text{CO}_2$  during the above-described months to simulated value solely to temperature effect (Figure 6a,c). In contrast, in Xiangyun station in urban constructed wetland, aquatic photosynthesis dominated the monthly variability of riverine  $p\text{CO}_2$  (Figure 6d), and from July to October with AOU of  $< -80 \mu\text{mol kg}^{-1}$  the station even acted as an atmospheric  $\text{CO}_2$  sink.

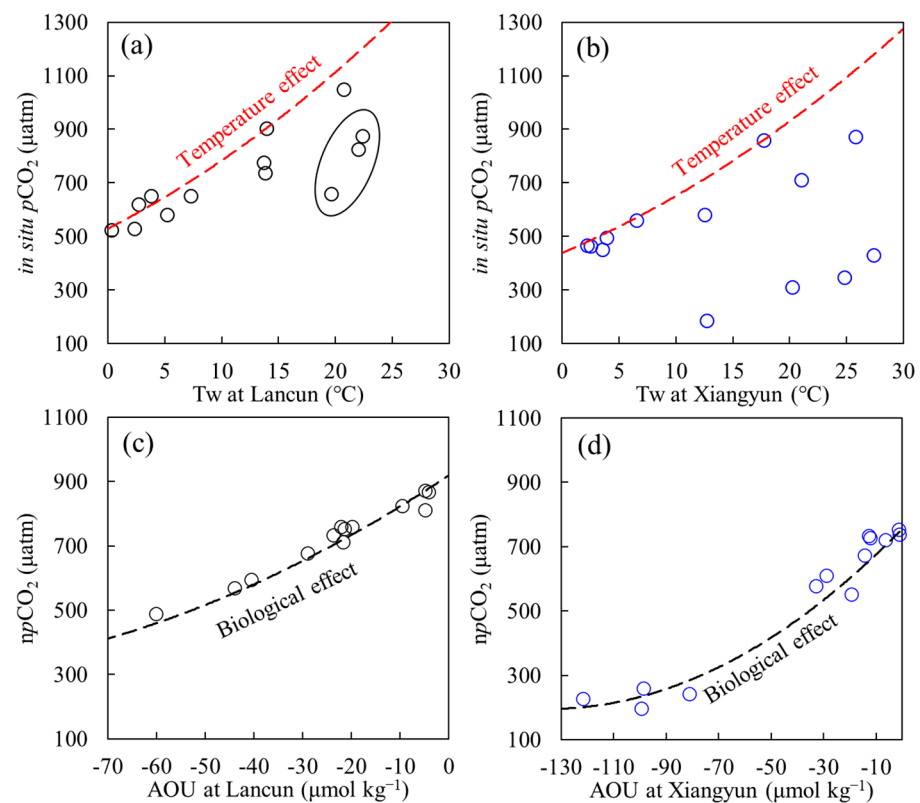


**Figure 6.** Plots of *in situ*  $p\text{CO}_2$  versus  $T_w$  and  $np\text{CO}_2$  versus AOU at Lancun station (a,c) and Xiangyun station (b,d). In panels (a,b), the dashed red line represents the variations of simulated  $p\text{CO}_2$  solely due to the temperature effect, starting from the value in May 2020. In panel (a), the values in black circle represent the observations from July to September. In panels (c,d), the dashed black line represents  $np\text{CO}_2$  variations just due to biological activities, which were determined based on the classic Redfield stoichiometry of  $\text{DIC}:\text{AOU} = 106:138$  and started from the value in May 2020.

In addition, some other factors may also affect the changes in  $p\text{CO}_2$ . Such as discharge and wind speed whose impacts are mainly reflected in the  $\text{CO}_2$  degassing process [66,67].

High discharge often enhances water-gas CO<sub>2</sub> exchange, promoting CO<sub>2</sub> degassing and leading to a decrease in *p*CO<sub>2</sub>. However, in Lancun station having good liquidity, we did not find an obvious decrease in *p*CO<sub>2</sub> in cold months (e.g., January and February) with high discharge compared with the warm months (e.g., July–October) with low discharge (Figure 2c,i). Especially the temperature normalized *p*CO<sub>2</sub> (*np*CO<sub>2</sub>) showed good agreement with biological Redfield line (Figure 6c). This indicated that discharge may have a minor effect on the monthly changes of *p*CO<sub>2</sub> at Lancun station. In comparison, in Xiangyun station with a nearly stationary water body, wind speed is an important factor affecting CO<sub>2</sub> degassing. However, it may also have a minor effect on *p*CO<sub>2</sub> monthly variation due to the *p*CO<sub>2</sub> levels (450 μatm, Figure 2j) close to atmospheric CO<sub>2</sub> and the good agreement between *np*CO<sub>2</sub> and simulated biological *p*CO<sub>2</sub> (Figure 6d). Nevertheless, the impact of CO<sub>2</sub> degassing on the changes of *p*CO<sub>2</sub> in rivers is still worth further research [3], especially quantifying their contributions will help to detail the specific impacts of important processes through calculation model or field experiments.

Overall, urban constructed wetlands can substantially contribute to the decrease in riverine CO<sub>2</sub> and even trigger the appearance of CO<sub>2</sub> sink. Urban constructed wetlands are capable of beautifying the residential environment and ecological landscape while bringing a vital natural CO<sub>2</sub> sink. Carbon reduction caused by constructed wetlands would become an important aspect of urban low-carbon management. Thus, supplemented by relevant protection policies and pollution discharge restrictions, expanding the scope of riverside wetlands along the river would be an effective low-carbon approach. This is due to the fact that urban wetlands not only bring ecological landscapes and a healthy environment to residents, but also promote low-carbon development and healthy management of cities. Moreover, the CO<sub>2</sub> absorption capacity arising from aquatic photosynthesis turned out to be a major underestimation factor of carbon sinks in rivers, especially in several non-free flowing rivers exhibiting highly eutrophic state [10,60,68]. Despite the rising attention aroused by the CO<sub>2</sub> sink in lakes that is caused by photosynthesis [69], the focus on urban wetland in the inland rivers has been limited (e.g., this study area). It is noteworthy that net autotrophic status even appeared in some forested headwater stream with a significant solar radiation and moderate temperature [70]. With the global expanding of urban area and rapid migration of population (over two thirds of the world's population was expected to cities by 2050) to big cities [71], the expected large CO<sub>2</sub> absorption from the atmosphere and carbon sequestration by urban eutrophic river reaches should be reviewed in depth. Moreover, compared with the humid areas and tropical rainforests, arid and semi-arid areas which covered 45% of global land surface had a higher turnover rates of carbon pools [72]. Notably, Ran et al. [3] suggested that the CO<sub>2</sub> emission of rivers in arid and semi-arid North and Northwestern China declined by 56% under the effects of damming and water withdrawals from the 1980s to the 2010s. Thus, more observation and targeted research on CO<sub>2</sub> systems should be conducted for urban rivers in arid and semi-arid regions in subsequent research.

#### 4.4. Limitation and Future Research

Some limitations and future research in this study were addressed. First, *p*CO<sub>2</sub> was determined based on pH and DIC. Thus, the uncertainty of *p*CO<sub>2</sub> calculated from the pH and DIC was estimated as ~25 μatm via the CO2SYS program, given the uncertainty of ~0.06 mg L<sup>-1</sup> for DIC measurement and the uncertainty of ~0.01 for pH measurement. However, this uncertainty can be ignored due to the large monthly variation of *p*CO<sub>2</sub> in the investigated stations. Second, AOU was adopted to determine whether the water body was dominated by primary production or community respiration. Though the supersaturated DO and negative AOU as well as the variation of DOC and δ<sup>13</sup>C<sub>DIC</sub> at Xiangyun station located in the wetland area better suggested the dominance of aquatic production on DIC and *p*CO<sub>2</sub>, further incubation experiments or investigation of related biological parameters (e.g., chlorophyll *a* or nutrients) can be conducive to revealing the effect of aquatic photosynthesis in depth. Moreover, some *in situ* experiments of calcification

precipitation can further confirm the occurrence of calcium carbonate precipitation in urban wetland areas. Third, this study focused on the main factors of DIC and  $p\text{CO}_2$  variability through correlation analysis and semi-quantitative means. However, some other processes (e.g., nitrification processes) may exist though their effects may be minor. Further, recently the interaction conversion between biological organic carbon and DIC was reported by Ni and Li [73] in detail. This process may also have a certain impact on riverine carbonate system indirectly in constructed wetland though more observations and profound explorations are still needed. Lastly, for the entire riverside constructed wetland, the change of carbonate system in different regions is still in doubt due to the limited investigated stations. Moreover, monthly observations for only one year cycle are limited due to the large annual changes of discharge. For example, in 2021 the annual discharge of the Fenhe River was  $16.65 \times 10^8 \text{ m}^3$ , which was obviously higher than the multi-year average value of  $9.18 \times 10^8 \text{ m}^3$  [31], and high discharge may lead to an underestimation of observed results due to dilution effect.

Correspondingly, further future research is urgently needed. Firstly, more field investigation (especially high frequency and continuous observation) will help to truly understand the real-time changes of  $\text{CO}_2$  systems in artificial wetland regions, and further accurately obtain  $\text{CO}_2$  flux to avoid missing unexpected events such as rainfall. Secondly, the observation of *in situ*  $p\text{CO}_2$  associated with laboratory cultivation experiments or *in situ* experiments [20], and the application of more advanced means about carbon cycle models will gain a deeper understanding of the internal mechanisms of biological process effects on riverine  $\text{CO}_2$  and to gain more insights into the complex  $\text{CO}_2$  system in urbanized rivers. Thirdly, this study confirms the carbon sequestration effect of constructed wetlands on  $\text{CO}_2$  absorption. In comparison, methane is also another important greenhouse gas associated with wetlands [23]. Relevant investigations combined with sediment and microbial analysis [74] will help us gain a more comprehensive understanding of the role of artificial wetlands in the entire river carbon system.

## 5. Conclusions

In this study, we analyzed the effect of constructed wetland on carbonate system in urbanized river based on monthly observations over an annual cycle from May 2020 to May 2021 at two compared stations, which were in a constructed wetland (Xiangyun station) and its upstream (Lancun station) in the Taiyuan section of the Fenhe River on the Loess Plateau. In Lancun station, riverine DIC and  $p\text{CO}_2$  were  $30.9\text{--}46.7 \text{ mg L}^{-1}$  and  $524\text{--}1050 \text{ }\mu\text{atm}$ , respectively. Its DIC was mainly sourced from natural carbonate weathering involved by  $\text{H}_2\text{CO}_3$  and  $\text{H}_2\text{SO}_4$  and discharge-affected weathering intensity dominated DIC seasonality while  $p\text{CO}_2$  was dominated by temperature. In comparison, a significant decrease in DIC and  $p\text{CO}_2$  was reported in Xiangyun station in constructed wetland, and the values reached  $24.1\text{--}39.1 \text{ mg L}^{-1}$  and  $188\text{--}873 \text{ }\mu\text{atm}$ , respectively. The above-mentioned decrease in DIC primarily arose from significant aquatic photosynthesis and calcification precipitation, whereas the decrease in  $p\text{CO}_2$  was attributed to aquatic photosynthesis that dominated the seasonality of  $p\text{CO}_2$ .

As revealed by the results of this study, urban constructed wetlands can notably contribute to the decrease in riverine  $\text{CO}_2$  and even trigger the appearance of  $\text{CO}_2$  sink. In urbanized semi-arid areas similar to the study area, scarce water resources are often efficiently utilized through dam or weir interception. More importantly, constructed wetlands could be set up to optimize water quality and living environments, becoming a natural driving force for urban low-carbon and sustainable development. With the increasing global  $\text{CO}_2$  concentration and urbanization especially the arid and semi-arid areas covering 45% of global land, aquatic photosynthesis and related biological processes caused by damming and constructed wetland resulted from population concentration will be even more important to the  $\text{CO}_2$  system in inland rivers. Thus, the  $\text{CO}_2$  absorption capacity arising from aquatic photosynthesis will become a major underestimation factor of  $\text{CO}_2$  sinks in urbanized rivers for  $\text{CO}_2$  neutralization.

**Author Contributions:** Conceptualization, Investigation, Software, Supervision, Writing—Original Draft, Writing—Review and Editing, J.D. and Y.L.; Formal analysis, Methodology, J.D., M.Z. and Y.L.; Funding acquisition, Y.L. All authors have read and agreed to the published version of the manuscript.

**Funding:** This research was funded by jointly supported by the Plan Project of Shanxi Basic Research, grant number 20210302124317, the Water Conservancy Science and Technology Research and Promotion Project in Shanxi, grant number 2023GM41, and the Scientific and Technological Innovation Programs of Higher Education Institutions in Shanxi, grant number 2020L0151.

**Data Availability Statement:** The data presented in this study are available on request from the corresponding author.

**Conflicts of Interest:** The authors declare no conflicts of interest.

## References

1. Barnes, R.T.; Raymond, P.A. The contribution of agricultural and urban activities to inorganic carbon fluxes within temperate watersheds. *Chem. Geol.* **2009**, *266*, 318–327. [[CrossRef](#)]
2. Chaplot, V.; Mutema, M. Sources and main controls of dissolved organic and inorganic carbon in river basins: A worldwide meta-analysis. *J. Hydrol.* **2021**, *603*, 126941. [[CrossRef](#)]
3. Ran, L.; Butman, D.E.; Battin, T.J.; Yang, X.; Tian, M.; Duvert, C.; Hartmann, J.; Geeraert, N.; Liu, S. Substantial decrease in CO<sub>2</sub> emissions from Chinese inland waters due to global change. *Nat. Commun.* **2021**, *12*, 1730. [[CrossRef](#)] [[PubMed](#)]
4. Raymond, P.A.; Hartmann, J.; Lauerwald, R.; Sobek, S.; McDonald, C.; Hoover, M.; Butman, D.; Striegl, R.; Mayorga, E.; Humborg, C.; et al. Global carbon dioxide emissions from inland waters. *Nature* **2013**, *503*, 355–359. [[CrossRef](#)]
5. Wehrli, B. Biogeochemistry: Conduits of the carbon cycle. *Nature* **2013**, *503*, 346–347. [[CrossRef](#)]
6. Lauerwald, R.; Hartmann, J.; Moosdorf, N.; Kempe, S.; Raymond, P.A. What controls the spatial patterns of the riverine carbonate system?—A case study for North America. *Chem. Geol.* **2013**, *337–338*, 114–127.
7. Reiman, J.H.; Xu, Y.J. Dissolved carbon export and CO<sub>2</sub> outgassing from the lower Mississippi River—Implications of future river carbon fluxes. *J. Hydrol.* **2019**, *578*, 124093. [[CrossRef](#)]
8. Zhang, F.; Xiao, X.; Wang, L.; Zeng, C.; Yu, Z.; Wang, G.; Shi, X. Chemical weathering and CO<sub>2</sub> consumption in the glaciated Karuxung River catchment, Tibetan Plateau. *Hydrol. Process* **2021**, *35*, e14330. [[CrossRef](#)]
9. Zhang, Q.; Jin, Z.; Zhang, F.; Xiao, J. Seasonal variation in river water chemistry of the middle reaches of the Yellow River and its controlling factors. *J. Geochem. Explor.* **2015**, *156*, 101–113. [[CrossRef](#)]
10. Chen, S.; Zhong, J.; Li, S.; Ran, L.; Wang, W.; Xu, S.; Yan, Z.; Xu, S. Multiple controls on carbon dynamics in mixed karst and non-karst mountainous rivers, Southwest China, revealed by carbon isotopes ( $\delta^{13}\text{C}$  and  $\Delta^{14}\text{C}$ ). *Sci. Total Environ.* **2021**, *791*, 148347. [[CrossRef](#)]
11. Wang, J.; Wang, X.; Liu, T.; Yuan, X.; Chen, H.; He, Y.; Wu, S.; Yuan, Z.; Li, H.; Que, Z.; et al. pCO<sub>2</sub> and CO<sub>2</sub> evasion from two small suburban rivers: Implications of the watershed urbanization process. *Sci. Total Environ.* **2021**, *788*, 147787. [[CrossRef](#)] [[PubMed](#)]
12. Zhong, J.; Li, S.L.; Cai, H.M.; Yue, F.J.; Tao, F.X. The response of carbon geochemistry to hydrological events within an urban river, Southwestern China. *Geochem. Int.* **2018**, *56*, 462–473. [[CrossRef](#)]
13. Li, S.; Luo, J.; Wu, D.; Jun Xu, Y. Carbon and nutrients as indicators of daily fluctuations of pCO<sub>2</sub> and CO<sub>2</sub> flux in a river draining a rapidly urbanizing area. *Ecol. Indic.* **2020**, *109*, 105821. [[CrossRef](#)]
14. Tang, W.; Jun Xu, Y.; Li, S. Rapid urbanization effects on partial pressure and emission of CO<sub>2</sub> in three rivers with different urban intensities. *Ecol. Indic.* **2021**, *125*, 107515. [[CrossRef](#)]
15. Yu, S.; He, S.; Sun, P.A.; Pu, J.; Huang, J.; Luo, H.; Li, Y.; Li, R.; Yuan, Y. Impacts of anthropogenic activities on weathering and carbon fluxes: A case study in the Xijiang River basin, southwest China. *Environ. Earth Sci.* **2016**, *75*, 589. [[CrossRef](#)]
16. Park, J.; Jin, H.; Yoon, T.K.; Begum, M.S.; Eliyan, C.; Lee, E.; Lee, S.; Oh, N. Wastewater-boosted biodegradation amplifying seasonal variations of pCO<sub>2</sub> in the Mekong-Tonle Sap river system. *Biogeochemistry* **2021**, *155*, 219–235. [[CrossRef](#)]
17. Yoon, T.K.; Jin, H.; Begum, M.S.; Kang, N.; Park, J. CO<sub>2</sub> outgassing from an urbanized river system fueled by wastewater treatment plant effluents. *Environ. Sci. Technol.* **2017**, *51*, 10459–10467. [[CrossRef](#)]
18. Vymazal, J. Enhancing ecosystem services on the landscape with created, constructed and restored wetlands. *Ecol. Eng.* **2011**, *37*, 1–5. [[CrossRef](#)]
19. Zhang, T.; Xu, D.; He, F.; Zhang, Y.; Wu, Z. Application of constructed wetland for water pollution control in China during 1990–2010. *Ecol. Eng.* **2012**, *47*, 189–197. [[CrossRef](#)]
20. Scholz, C.; Jones, T.G.; West, M.; Ehbair, A.M.S.; Dunn, C.; Freeman, C. Constructed wetlands may lower inorganic nutrient inputs but enhance DOC loadings into a drinking water reservoir in North Wales. *Environ. Sci. Pollut. Res.* **2016**, *23*, 18192–18199. [[CrossRef](#)]
21. Zhao, C.; Xu, J.; Shang, D.; Zhang, Y.; Zhang, J.; Xie, H.; Kong, Q.; Wang, Q. Application of constructed wetlands in the PAH remediation of surface water: A review. *Sci. Total Environ.* **2021**, *780*, 146605. [[CrossRef](#)]

22. Rizzo, A.; Tondera, K.; Pálffy, T.G.; Dittmer, U.; Meyer, D.; Schreiber, C.; Zacharias, N.; Ruppelt, J.P.; Esser, D.; Molle, D.; et al. Constructed wetlands for combined sewer over flow treatment: A state-of-the-art review. *Sci. Total Environ.* **2020**, *727*, 138618. [[CrossRef](#)]
23. de Klein, J.J.M.; van der Werf, A.K. Balancing carbon sequestration and GHG emissions in a constructed wetland. *Ecol. Eng.* **2014**, *66*, 36–42. [[CrossRef](#)]
24. Schäfer, K.V.R.; Tripathee, R.; Artigas, F.; Morin, T.H.; Bohrer, G. Carbon dioxide fluxes of an urban tidal marsh in the Hudson-Raritan estuary. *J. Geophys. Res. Biogeosci.* **2014**, *119*, 2065–2081. [[CrossRef](#)]
25. Wu, Y.; Mao, X.; Zhang, Z.; Tang, W.; Cao, G.; Zhou, H.; Ma, J.; Yin, X. Temporal and spatial characteristics of CO<sub>2</sub> flux in plateau urban wetlands and their influencing factors based on eddy covariance technique. *Water* **2021**, *13*, 1176. [[CrossRef](#)]
26. Zhang, H.; Tang, W.; Wang, W.; Yin, W.; Liu, H.; Ma, X.; Zhou, Y.; Lei, P.; Wei, D.; Zhang, L.; et al. A review on China's constructed wetlands in recent three decades: Application and practice. *J. Environ. Sci.* **2021**, *104*, 53–68. [[CrossRef](#)]
27. Cai, W.; Guo, X.; Chen, C.A.; Dai, M.; Zhang, L.; Zhai, W.; Lohrenz, S.E.; Yin, K.; Harrison, P.J.; Wang, Y. A comparative overview of weathering intensity and HCO<sub>3</sub><sup>−</sup> flux in the world's major rivers with emphasis on the Changjiang, Huanghe, Zhujiang (Pearl) and Mississippi Rivers. *Cont. Shelf Res.* **2008**, *28*, 1538–1549. [[CrossRef](#)]
28. Wang, X.; Luo, C.; Ge, T.; Xu, C.; Xue, Y. Controls on the sources and cycling of dissolved inorganic carbon in the Changjiang and Huanghe River estuaries, China: <sup>14</sup>C and <sup>13</sup>C studies. *Limnol. Oceanogr.* **2016**, *61*, 1358–1374. [[CrossRef](#)]
29. Shan, S.; Luo, C.; Qi, Y.; Cai, W.; Sun, S.; Fan, D.; Wang, X. Carbon isotopic and lithologic constraints on the sources and cycling of inorganic carbon in four large rivers in China: Yangtze, Yellow, Pearl, and Heilongjiang. *J. Geophys. Res. Biogeo.* **2021**, *126*, e2020JG005901. [[CrossRef](#)]
30. Wu, W. Hydrochemistry of inland rivers in the north Tibetan Plateau: Constraints and weathering rate estimation. *Sci. Total Environ.* **2016**, *541*, 468–482. [[CrossRef](#)] [[PubMed](#)]
31. Department of Ecological Environment of Shanxi Province. *Report on the Ecological Environment of Shanxi Province in 2021*; Department of Ecological Environment of Shanxi Province: Taiyuan, China, 2021.
32. Yang, Y.; Meng, Z.; Jiao, W. Hydrological and pollution processes in mining area of Fenhe River Basin in China. *Environ. Pollut.* **2018**, *234*, 743–750. [[CrossRef](#)] [[PubMed](#)]
33. Grasshoff, K.; Kremling, K.; Ehrhardt, M. *Methods of Seawater Analysis*, 3rd ed.; Wiley: Weinheim, Germany, 1999.
34. Liu, Z.; Zhang, L.; Cai, W.; Wang, L.; Xue, M.; Zhang, X. Removal of dissolved inorganic carbon in the Yellow River Estuary. *Limnol. Oceanogr.* **2014**, *59*, 413–426. [[CrossRef](#)]
35. Xue, L.; Yang, X.; Li, Y.; Li, L.; Jiang, L.; Xin, M.; Wang, Z.; Sun, X.; Wei, Q. Processes controlling sea surface pH and aragonite saturation state in a large northern temperate bay: Contrasting temperature effects. *J. Geophys. Res. Biogeo.* **2020**, *125*, e2020JG005805. [[CrossRef](#)]
36. Zhang, T.; Li, J.; Pu, J.; Yuan, D. Carbon dioxide exchanges and their controlling factors in Guijiang River, SW China. *J. Hydrol.* **2019**, *578*, 124073. [[CrossRef](#)]
37. Li, Y.; Yang, H.; Dang, J.; Yang, X.; Xue, L.; Zhang, L. Seasonal variation of sea surface pH and its controls in the Jiaozhou Bay, China. *Cont. Shelf Res.* **2022**, *232*, 104613. [[CrossRef](#)]
38. Lewis, E.; Wallace, D.W. *Program Developed for CO<sub>2</sub> Systems Calculations*; ORNL/CDIAC 105; Carbon Dioxide Information Analysis Center, Oak Ridge National Laboratory US Department of Energy: Oak Ridge, TN, USA, 1998.
39. Chen, B.; Cai, W.; Brodeur, J.R.; Hussain, N.; Testa, J.M.; Ni, W.; Li, Q. Seasonal and spatial variability in surface pCO<sub>2</sub> and air-water CO<sub>2</sub> flux in the Chesapeake Bay. *Limnol. Oceanogr.* **2020**, *65*, 3046–3065. [[CrossRef](#)]
40. Millero, F.J. The thermodynamics of the carbonate system in seawater. *Geochim. Cosmochim. Acta* **1979**, *43*, 1651–1661. [[CrossRef](#)]
41. Redfield, A.C. The influence of organisms on the composition of seawater. *Sea* **1963**, *2*, 26–77.
42. Calabrese, S.; Parolari, A.J.; Porporato, A. Hydrologic transport of dissolved inorganic carbon and its control on chemical weathering. *J. Geophys. Res. Earth* **2017**, *122*, 2016–2032. [[CrossRef](#)]
43. Sun, P.; He, S.; Yu, S.; Pu, J.; Yuan, Y.; Zhang, C. Dynamics in riverine inorganic and organic carbon based on carbonate weathering coupled with aquatic photosynthesis in a karst catchment, Southwest China. *Water Res.* **2021**, *189*, 116658. [[CrossRef](#)]
44. Meybeck, M. Global chemical weathering of surficial rocks estimated from river dissolved loads. *Am. J. Sci.* **1987**, *287*, 401–428. [[CrossRef](#)]
45. Martin, J.B. Carbonate minerals in the global carbon cycle. *Chem. Geol.* **2017**, *449*, 58–72. [[CrossRef](#)]
46. Clark, I.D.; Fritz, P. *Environmental Isotopes in Hydrogeology*; Lewis Publishers: New York, NY, USA, 1997; pp. 111–169.
47. Deuser, W.G.; Degens, E.T. Carbon isotope fractionation in the system CO<sub>2</sub>(gas)-CO<sub>2</sub>(aqueous)-HCO<sub>3</sub><sup>−</sup>(aqueous). *Nature* **1967**, *215*, 1033–1035. [[CrossRef](#)]
48. Telmer, K.; Veizer, J. Carbon fluxes, pCO<sub>2</sub> and substrate weathering in a large northern river basin, Canada: Carbon isotope perspectives. *Chem. Geol.* **1999**, *159*, 61–86. [[CrossRef](#)]
49. National Bureau of Statistics of China. *China Statistical Yearbook 2021*; National Bureau of statistics of China: Beijing, China, 2021.
50. Zhang, Y.; Jiang, Y.; Yuan, D.; Cui, J.; Li, Y.; Yang, J.; Cao, M. Source and flux of anthropogenically enhanced dissolved inorganic carbon: A comparative study of urban and forest karst catchments in Southwest China. *Sci. Total Environ.* **2020**, *725*, 138255. [[CrossRef](#)]
51. Wang, W.; Li, S.; Zhong, J.; Li, C.; Yi, Y.; Chen, S.; Ren, Y. Understanding transport and transformation of dissolved inorganic carbon (DIC) in the reservoir system using δ<sup>13</sup>C<sub>DIC</sub> and water chemistry. *J. Hydrol.* **2019**, *574*, 193–201. [[CrossRef](#)]

52. Jiang, D.; Li, Z.; Luo, Y.; Xia, Y. River damming and drought affect water cycle dynamics in an ephemeral river based on stable isotopes: The Dagu River of North China. *Sci. Total Environ.* **2021**, *758*, 143682. [[CrossRef](#)]
53. Maavara, T.; Lauerwald, R.; Regnier, P.; Van Cappellen, P. Global perturbation of organic carbon cycling by river damming. *Nat. Commun.* **2017**, *8*, 15347. [[CrossRef](#)]
54. Ran, L.; Li, L.; Tian, M.; Yang, X.; Yu, R.; Zhao, J.; Wang, L.; Lu, X.X. Riverine CO<sub>2</sub> emissions in the Wuding River catchment on the Loess Plateau: Environmental controls and dam impoundment impact. *J. Geophys. Res. Biogeo.* **2017**, *122*, 1439–1455. [[CrossRef](#)]
55. Cui, G.; Li, X.; Li, Q.; Huang, J.; Tao, Y.; Li, S.; Zhang, J. Damming effects on dissolved inorganic carbon in different kinds of reservoirs in Jialing River, Southwest China. *Acta Geochim.* **2017**, *36*, 581–597. [[CrossRef](#)]
56. Wang, W.; Li, S.; Zhong, J.; Maberly, S.C.; Li, C.; Wang, F.; Xiao, H.; Liu, C. Climatic and anthropogenic regulation of carbon transport and transformation in a karst river-reservoir system. *Sci. Total Environ.* **2020**, *707*, 135628. [[CrossRef](#)]
57. Cicerone, D.S.; Stewart, A.J.; Roh, Y. Diel cycles in calcite production and dissolution in a eutrophic basin. *Environ. Toxicol. Chem.* **1999**, *18*, 2169–2177. [[CrossRef](#)]
58. Hammes, F.; Verstraete, W. Key roles of pH and calcium metabolism in microbial carbonate precipitation. *Rev. Environ. Sci. Biotechnol.* **2002**, *1*, 3–7. [[CrossRef](#)]
59. Liu, Z.; Macpherson, G.L.; Groves, C.; Martin, J.B.; Yuan, D.; Zeng, S. Large and active CO<sub>2</sub> uptake by coupled carbonate weathering. *Earth-Sci. Rev.* **2018**, *182*, 42–49. [[CrossRef](#)]
60. Rogerson, M.; Pedley, H.M.; Wadhawan, J.D.; Middleton, R. New insights into biological influence on the geochemistry of freshwater carbonate deposits. *Geochim. Cosmochim. Acta* **2008**, *72*, 4976–4987. [[CrossRef](#)]
61. de Montety, V.; Martin, J.B.; Cohen, M.J.; Foster, C.; Kurz, M.J. Influence of diel biogeochemical cycles on carbonate equilibrium in a karst river. *Chem. Geol.* **2011**, *283*, 31–43. [[CrossRef](#)]
62. Yang, M.; Liu, Z.; Sun, H.; Yang, R.; Chen, B. Organic carbon source tracing and DIC fertilization effect in the Pearl River: Insights from lipid biomarker and geochemical analysis. *Appl. Geochem.* **2016**, *73*, 132–141. [[CrossRef](#)]
63. Zhang, J.; Liu, M.G. Observations on nutrient elements and sulphate in atmospheric wet depositions over the northwest Pacific coastal oceans—Yellow Sea. *Mar. Chem.* **1994**, *47*, 173–189. [[CrossRef](#)]
64. Zhang, G.; Zhang, J.; Liu, S. Characterization of nutrients in the atmospheric wet and dry deposition observed at the two monitoring sites over Yellow Sea and East China Sea. *J. Atmos. Chem.* **2007**, *57*, 41–57. [[CrossRef](#)]
65. Weiss, R.F. Carbon dioxide in water and seawater: The solubility of a non-ideal gas. *Mar. Chem.* **1974**, *2*, 203–215. [[CrossRef](#)]
66. Xia, M.; Craig, P.M.; Schaeffer, B.; Stoddard, A.; Liu, Z.; Peng, M.; Zhang, H.; Wallen, C.M.; Bailey, N.; Mandrup-Poulsen, J. Influence of physical forcing on bottom-water dissolved oxygen within Caloosahatchee River Estuary, Florida. *J. Environ. Eng.* **2010**, *136*, 1032–1044. [[CrossRef](#)]
67. Liu, Y.; Weisberg, R.H.; Zheng, L.; Heil, C.A.; Hubbard, K.A. Termination of the 2018 Florida red tide event: A tracer model perspective. *Estuar. Coast. Shelf Sci.* **2022**, *272*, 107901. [[CrossRef](#)]
68. Grill, G.; Lehner, B.; Thieme, M.; Geenen, B.; Tickner, D.; Antonelli, F.; Babu, S.; Borrelli, P.; Cheng, L.; Crochetiere, H.; et al. Mapping the world's free-flowing rivers. *Nature* **2019**, *569*, 215–221. [[CrossRef](#)]
69. Pacheco, F.S.; Roland, F.; Downing, J.A. Eutrophication reverses whole-lake carbon budgets. *Inland Waters* **2014**, *4*, 41–48. [[CrossRef](#)]
70. Roberts, B.J.; Mulholland, P.J.; Hill, W.R. Multiple scales of temporal variability in ecosystem metabolism rates: Results from 2 years of continuous monitoring in a forested headwater stream. *Ecosystems* **2007**, *10*, 588–606. [[CrossRef](#)]
71. Gratani, L.; Catoni, R.; Puglielli, G.; Varone, L.; Crescente, M.F.; Sangiorgio, S.; Lucchetta, F. Carbon dioxide (CO<sub>2</sub>) sequestration and air temperature amelioration provided by urban parks in Rome. *Energy Procedia* **2016**, *101*, 408–415. [[CrossRef](#)]
72. Poulter, B.; Frank, D.; Ciais, P.; Myneni, R.B.; Andela, N.; Bi, J.; Broquet, G.; Canadell, J.G.; Chevallier, F.; Liu, Y.Y.; et al. Contribution of semi-arid ecosystems to interannual variability of the global carbon cycle. *Nature* **2014**, *509*, 600–603. [[CrossRef](#)]
73. Ni, M.; Li, S. Dynamics and internal links of dissolved carbon in a karst river system: Implications for composition, origin and fate. *Water Res.* **2022**, *226*, 119289. [[CrossRef](#)]
74. Bledsoe, R.B.; Bean, E.Z.; Austin, S.S.; Peralta, A.L. A microbial perspective on balancing trade-offs in ecosystem functions in a constructed stormwater wetland. *Ecol. Eng.* **2020**, *158*, 109000. [[CrossRef](#)]

**Disclaimer/Publisher's Note:** The statements, opinions and data contained in all publications are solely those of the individual author(s) and contributor(s) and not of MDPI and/or the editor(s). MDPI and/or the editor(s) disclaim responsibility for any injury to people or property resulting from any ideas, methods, instructions or products referred to in the content.